Arch. Metall. Mater. **64** (2019), 1, 227-233

DOI: 10.24425/amm.2019.126242

D. BOCHENEK*, P. NIEMIEC*#, M. ADAMCZYK*, Z. STOKŁOSA**

ELECTROPHYSICAL PROPERTIES OF THE MULTICOMPONENT $PbFe_{1/2}Nb_{1/2}O_3$ CERAMICS DOPED BY Li

The paper presents the results of research on the influence of sintering temperature on microstructure, DC electrical conductivity, dielectric, ferroelectric and magnetic properties of $PbFe_{1/2}Nb_{1/2}O_3$ ceramics doped by Li in the amount of 5.0% wt., in the abbreviation PLiFN. The ceramic samples of the PLiFN material were obtained by the two-stage synthesis – columbite method and sintered by free sintering methods. Introduction to the basic $PbFe_{1/2}Nb_{1/2}O_3$ composition of the lithium admixture to decrease the electrical conductivity and reduction of dielectric loss. The tests have shown that the increase in sintering temperature orders the PLiFN ceramic microstructure, which has a positive effect on its electrophysical properties. At room temperature, the PLiFN ceramic samples show both ferroelectric and ferromagnetic properties. Considering the functional parameters of the obtained ceramic samples, the optimal technological conditions are 1100°C/2 h.

Keywords: ferroelectromagnetic, multiferroics, PFN

1. Introduction

Multiferroics constitute narrow group of functional materials which demonstrate at least two types of physical states at the same time [1-3] i.e. a ferromagnetic (antiferromagnetic, ferrimagnetic), ferroelectric (antiferroelectric, ferrielectric), ferroelastic (ferromagnetoelastic, ferroelastoelectric), ferrotoroic orderings. The smart materials (multiferroics) are able to change their properties according to external factors and those changes remain after removing mentioned factors.

Ferroelectromagnetic $PbFe_{1-x}Nb_xO_3$ material belong to the perovskite-like family with the general formula $A(B¢B²)O_3$ [4-5]. The multiferroic $PbFe_{1/2}Nb_{1/2}O_3$ (PFN) material was first synthesized and described by Smolensky [6-7] and Venevcev [8]. This material is characterized by two ordered antiferromagnetic and ferroelectric subsystems (below -130°C). Above -130°C temperature is reported to show relaxor ferroelectricity [9-11]. Formation pyrochlore phase during technological process, excess of Pb lead as well as high electric conductivity are major application problems of the PFN ceramics (particularly in microelectronic and micromechatronic applications). These negative factors can be eliminated or minimized by doping the basic composition of the PFN, for example by Li [12-13]. Wide isomorphism occurring in PFN compound allows to substitute different cations to A and (or) B positions into elementary cell. The PFN ceramic powders will be obtained by two-stage method, conventional method, mechanochemical method, sol-gel method, solution precipitation method etc. [14-16].

Use of suitable admixtures during technology of the PFN ceramics can achieve materials with optimal complex of the parameters. These type materials in form simple composition, solid solutions and ceramic (polimer) composites may be used as a multilayer ceramic capacitors (MLCC) and inductors, multilayer microwave resonators and filters, transducers, pyroelectric sensors, electrostrictive actuators, micropositiometers and memory devices [17]. Materials exhibiting multiferroic properties can be designed and obtained in various forms (single crystals, polycrystalline ceramic materials, ceramic or polimer composites, thin films, multilayer materials etc.).

In present work the technology and complex of electrophysical and magnetic properties of the $PbFe_{1/2}Nb_{1/2}O_3$ material doped by Li were presented.

2. Experimental

The ceramic samples of the $PbFe_{1/2}Nb_{1/2}O_3$ material doped by Li (PLiFN) in the amount of 5.0% wt. were obtained by the two-stage synthesis (columbite method). In the first stage the $FeNbO_4$ component is obtained from a mixture of simple oxides Fe_2O_3 and Nb_2O_5 in the synthesis conditions: 1000°C/4 h. In the second stage three components PbO, Li_2CO_3 and $FeNbO_4$ in powders form were mixed in a planetary mill for 8 h. The milled powders were synthesized at T_{s2} = 800°C and t_{s2} = 3 h by calcination route. The final sintering (densification) of the ceramic samples PLiFN was conducted in the four different conditions:

* UNIVERSITY OF SILESIA IN KATOWICE, FACULTY OF COMPUTER SCIENCE AND MATERIAL SCIENCE, INSTITUTE OF TECHNOLOGY AND MECHATRONICS, 12, ŻYTNIA STR., 41–200, SOSNOWIEC, POLAND,

** UNIVERSITY OF SILESIA IN KATOWICE, FACULTY OF COMPUTER SCIENCE AND MATERIAL SCIENCE, INSTITUTE OF MATERIAL SCIENCE, 1A, 75 PUŁKU PIECHOTY STR., 41–500 CHORZÓW, POLAND

Corresponding author: przemyslaw.niemiec@us.edu.pl

(i) 950°C/2 h (PLiFN1), (ii) 1050°C/2 h (PLiFN2), (iii) 1100°C/2 h (PLiFN3), (iv) 1150°C/2 h (PLiFN4). On the both sides of surface ceramic PLiFN samples (in disc form with diameter 10 mm and thickness 1 mm) silver electrodes have been putted.

The X-ray testes were carried out using Philips X'Pert diffractometer. The SEM microstructural studies of ceramic sample breakthroughs and the EDS (Energy Dispersive Spectrometry) study were carried out by a JEOL JSM-7100F TTL LV Field Emission Scanning Electron Microscope. Dielectric measurements were carried out using the capacity bridge of a QuadTech 1920 Precision LCR Meter for a heating cycle (at frequencies of the measurement field from v = 0.02 kHz to 20 kHz). Ferroelectric hysteresis (P–E) loops at room temperature were investigated with a Sawyer-Tower circuit and a Matsusada Inc. HEOPS-5B6 precision high voltage amplifier. Data were stored on a computer disc using an A/D, D/A transducer card. The DC electrical conductivity has been measured using a Keithley 6517B electrometer in temperatures range from 20°C to 250°C. Magnetic properties were obtained by the Quantum Design PPMS system (Quantum Design, PPMS 7T ACMS module). Dynamic magnetic susceptibility (the real and imaginary part and magnetic loss) was measured versus the frequency of the magnetic field (ranging from 50 Hz to 2000 Hz, magnetic field 800 A/m). All magnetic measurements were carried out at room temperature.

3. Results and discussion

X-ray diffraction pattern for synthesized PLiFN powder is presented in Fig. 1. At the room temperature all maxima belong to the perovskite phase without the presence of the foreign pyrochlore phase ($Pb_2Nb_2O_7$). The pyrochlore phase in the materials with perovskite structure is often formed during the technological process. The X-ray pattern of the PLiFN powder is matching well with the tetragonal symmetry with P4mm space group (JCPDS card no. 04-009-5124).

The SEM images of the microstructure PLiFN ceramics sintering at different temperatures (950°C, 1050°C, 1100°C, 1150°C) are presented in Fig. 2. In case ceramics sintered in lower temperature (PLiFN1 sample, Fig. 2a) the fine-grained microstructure is shown and average grain size is in the range of 2-5 μm. For higher temperature treatments, almost clean microstructures with highly uniform, dense grain packing are generally found (it is seen highly dense grain-packing with thinner grain boundaries). Increase of the sintering temperature causes increase grains in microstructure of the ceramic samples.

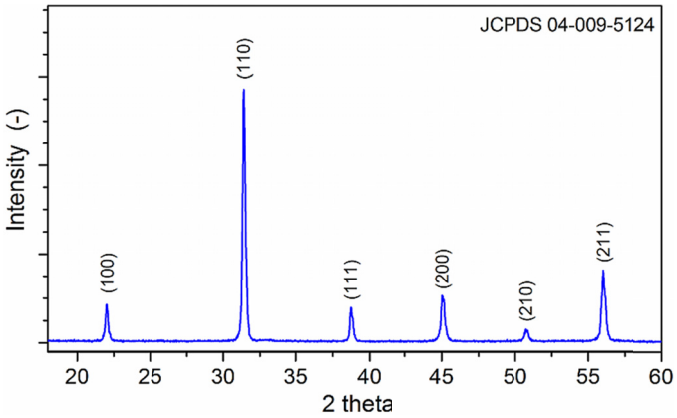

Fig. 1. X-ray spectra of the PLiFN powder

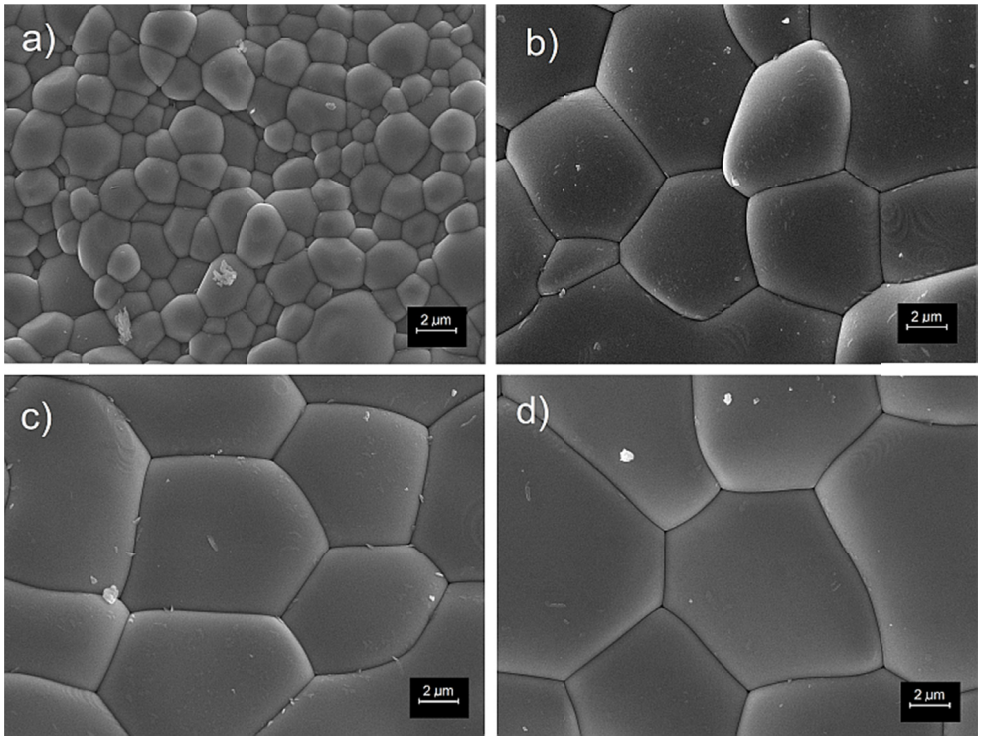

Fig. 2. SEM images of the microstructure PLiFN ceramics sintering at different temperatures: a) 950°C (PLiFN1), b) 1050°C (PLiFN2), c) 1100°C (PLiFN3), d) 1150°C (PLiFN4)

On the basis of the SEM images of the microstructures (Fig. 2b,c) it can be stated that in case ceramic samples sintered at temperature 1050°C and 1100°C (PLiFN2 and PLiFN3 samples), large heterogeneity of grain sizes takes place compared to the other samples. Its average grain size is in the range of 6-9 μm. There is an apparent increase in the average grain size (in the range of 8-14 μm) when the sintering temperature is raised to 1150°C (PLiFN4 sample).

The ionic radius of Li (0.90 Å) is too large for it to go onto the B-sites of the perovskite unit cell in compare others ions Fe (0.69 Å), Nb (0.78 Å) – based on the Shannon radii. The Goldschmidt tolerance factor *t* is often used to demonstrate the degree of distortion and suggest the stability of the perovskite structure [18]. Based on the tolerance factor calculated according formula:

$$t = \frac{R_A + R_O}{\sqrt{2}\left(R_B + R_O\right)} \tag{1}$$

were R_A is the ionic radii of the A-site cation, R_B, ionic radii of the B-site cation, and R_O is the ionic radii of the oxygen anion, the ionic radius of Li still is too large of the B-side perovskite unit cell. The doped lithium ions will be substituted in position A – in places occupied by lead ions Pb (1.33 Å). Due to the smaller ionic radiation, PFN doping with lithium will induce a local deformation of the crystalline structural in the form of network contraction.

The PFN ceramic samples were subjected to composition homogeneity tests by spectroscopy with EDS energy dispersion (Fig. 3) based on point and surface analysis. The EDS measurements confirmed the qualitative composition without the presence of foreign elements of the PFN samples. In the Table 1 was presented theoretical and calculated the percentage of the individual components of the PFN ceramics. In the case all samples, lead deficiency and a small excess of niobium are observed compared to theoretical calculations. All deviations from the PFN samples are within the acceptable range. In the case

TABLE 1

Theoretical and experimental percentages of elements (expressed as oxides) of PLiFN ceramics

Sample	**PLiFN**	**PLiFN1**	**PLiFN2**	**PLiFN3**	**PLiFN4**
T_s (°C)	—	**950**	**1050**	**1100**	**1150**
	Theoretical (%)	**Experimental (%)**	**Experimental (%)**	**Experimental (%)**	**Experimental (%)**
PbO	67.63	68.70	67.78	67.60	67.57
Fe_2O_3	12.09	11.62	12.37	12.41	12.56
Nb_2O_5	20.12	19.68	19.85	19.99	19.87
LiO	0.16	—	—	—	—

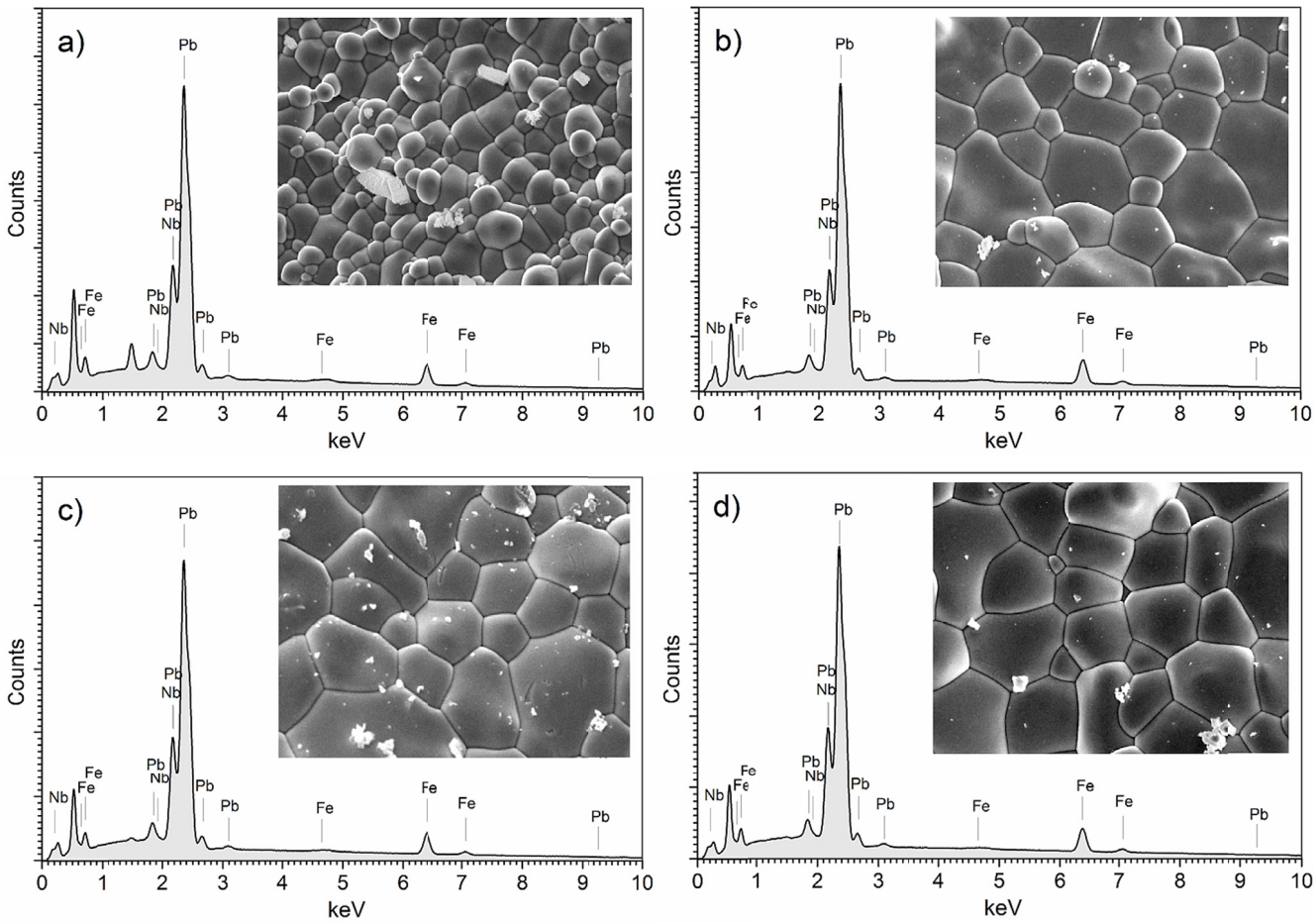

Fig. 3. EDS testes of the PFN samples: a) PLiFN1, b) PLiFN2, c) PLiFN3, d) PLiFN4

of the PLiFN1 sample a small excess of niobium are observed, too and the disproportions of the components in compare to theoretic calculations are the largest.

The temperature dependence of dielectric permittivity for PLiFN ceramics sintered at different temperatures is shown in Fig. 4. At room temperature (RT), the values of dielectric constant are for 2660, 2265, 2450 and 2305 for ceramic samples of the PLiFN1, PLiFN2, PLiFN3 and PLiFN4 respectively. In the case of low sintering temperature (for 950°C – Fig. 4a), the effect of dielectric loss on the value of dielectric permittivity is clear (it is clearly visible for the temperature area above the phase transition in the form of an additional maximum). Increasing the sintering temperature orders the crystalline structure of the PLiFN ceramics, which is manifested by reducing the phase transition broadening and minimizing the effect of the electrical conductivity on dielectric properties (for PLiFN3 – Fig. 4c). Temperature tests of dielectric properties also showed that increasing the sintering temperature slightly shifts the phase transition temperature towards lower temperatures. In order to evaluate the phase transition the modified Curie-Weiss law (2) was used

$$\frac{1}{\varepsilon}-\frac{1}{\varepsilon_m}=C\left(T-T_m\right)^{\alpha} \tag{2}$$

where: ε_m is the value of dielectric constant maximum, T_m the temperature of value of dielectric permittivity maximum, C represents Curie-Weiss parameter and α is the parameters indicating the degree of blur of the phase transition. When $\alpha = 1$ indicates normal Curie-Weiss behavior, while $\alpha = 2$ represents a relaxor phase transition. The α parameter was calculated by the slope of graph plotted between $\ln(1/\varepsilon - 1/\varepsilon_m)$ and $\ln(T - T_m)$ (not presented here) and is 1.56, 1.50, 1.66, and 1.82 for PLiFN1, PLiFN2, PLiFN3 and PLiFN4, respectively.

The temperature dependence of the tangent of the dielectric loss angle for PLiFN ceramics sintered at different temperatures is shown in Fig. 5. The increase in the synthesis temperature of the PLiFN ceramics contributes to the reduction of dielectric loss both at room temperature and at the phase transition temperature

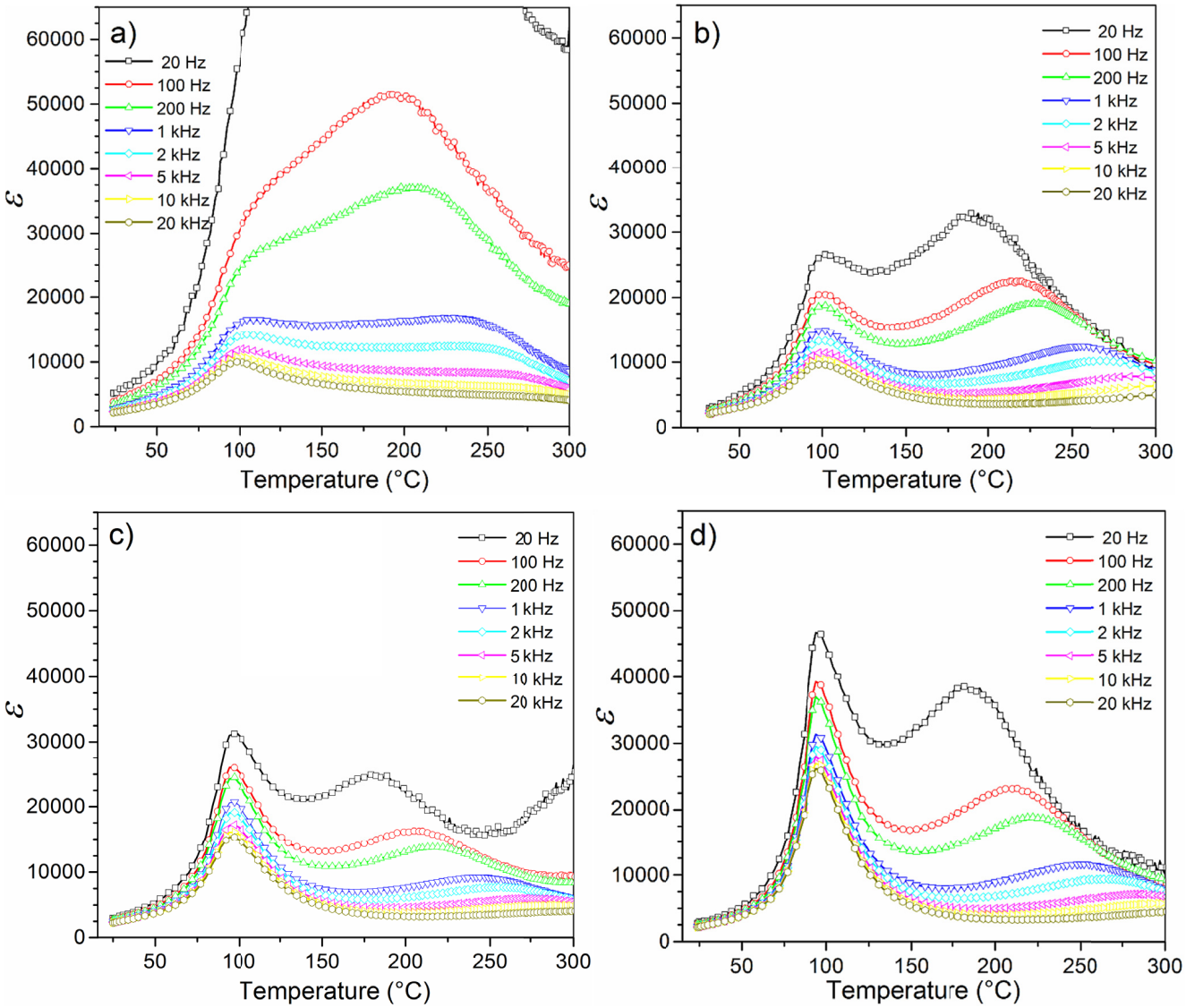

Fig. 4. The $\varepsilon(T)$ temperature relationships for the $PLi_{0.05}FN$ ceramics sintering at different temperatures: a) 950°C (PLiFN1), b) 1050°C (PLiFN2), c) 1100°C (PLiFN3), d) 1150°C (PLiFN4), at heating cycle

(Table 2) and the temperature plots show similarity. Above the phase transition temperature, a rapid increase in dielectric loss is observed associated with a significant increase in electrical conductivity. Taking into account the dielectric loss values, the most optimal sintering temperature is between 1050°C and 1100°C.

Fig. 6 shows the dependency of the $\ln\sigma(1/T)$ for PLiFN ceramics. Increase sintering temperature causes decrease of DC conductivity. Reduction of electrical conductivity in PLiFN ceramics obtained at higher sintering temperatures is also associated with well-formed microstructure, with densely packed grain and lower porosity. For the linear parts of $\ln\sigma(1/T)$ plots it was possible to calculate the activation energy from the Arrhenius formula:

$$\sigma = \sigma_0 e^{-\frac{E_a}{kT}} \tag{3}$$

where: σ – conductivity at given temperature, σ_0 – pre-exponential factor, E_a – activation energy, k – Boltzman constant, T – temperature. Calculated values of activation energy are presented in Table 2 and are of the same order as for example in works [19].

TABLE 2

The influence of the sintering temperature on the electrophysical parameters of the PLiFN ceramics

	PLiFN1	**PLiFN2**	**PLiFN3**	**PLiFN4**
T_s (°C)	950	1050	1100	1150
T_m (°C)	110	100	97	95
ε_r	2660	2265	2450	2302
ε_m	18598	14864	20786	31310
tanδ at RT	0.210	0.062	0.056	0.038
tanδ at T_m	0.639	0.241	0.168	0.144
E_{a1} (eV) at I range	0.545	0.678	0.629	0.677
E_{a2} (eV) at II range	0.715	0.615	0.823	0.490
E_{a3} (eV) at III range	0.650	0.760	0.744	0.765
P_r (μC/cm^2)	13.58	13.16	11.55	14.34
E_c (kV/mm)	0.40	0.38	0.50	0.300

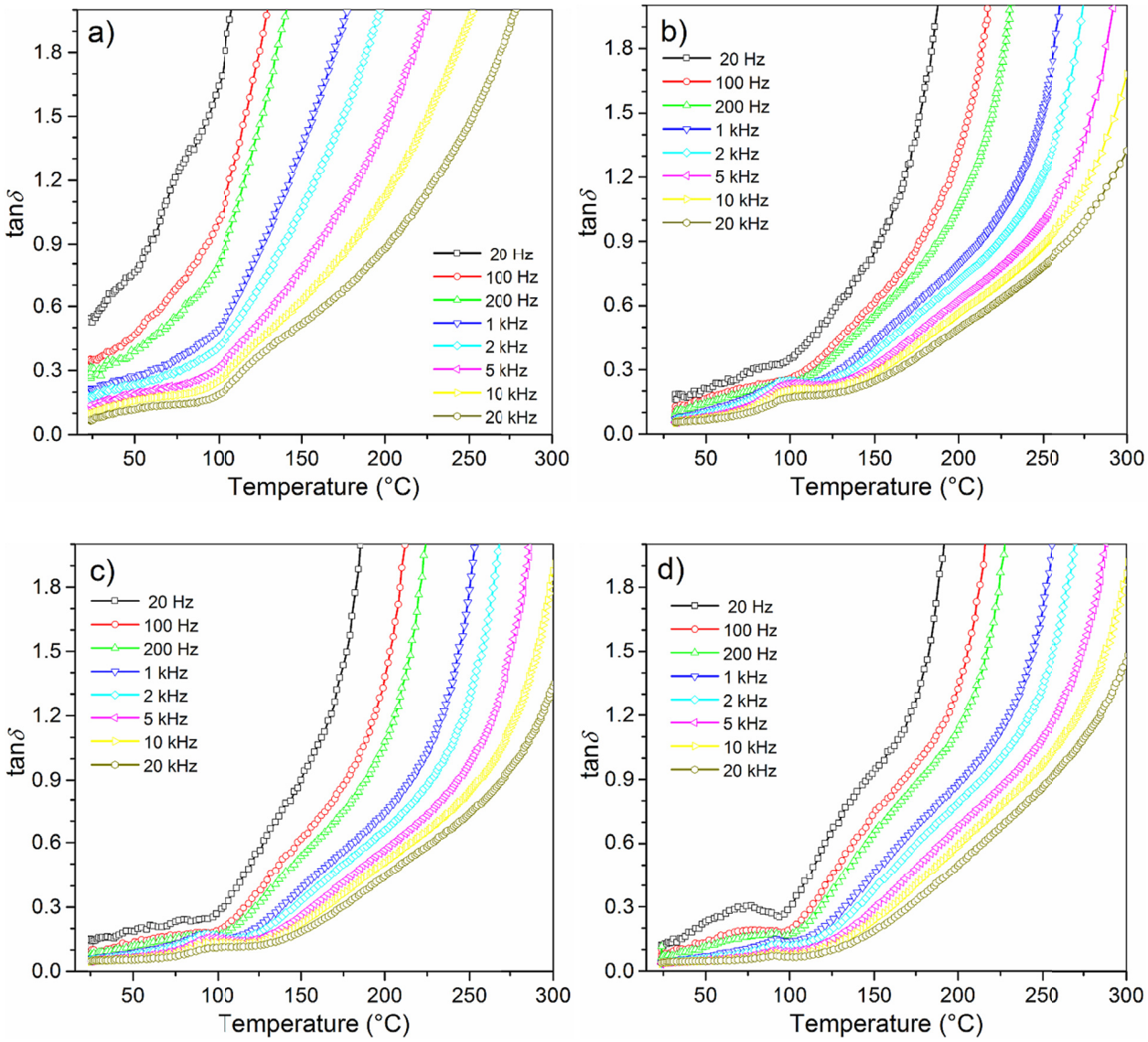

Fig. 5. Temperature dependencies of the tanδ for the PLiFN ceramics sintering at different temperatures: a) 950°C (PLiFN1), b) 1050°C (PLiFN2), c) 1100°C (PLiFN3), d) 1150°C (PLiFN4), at heating cycle

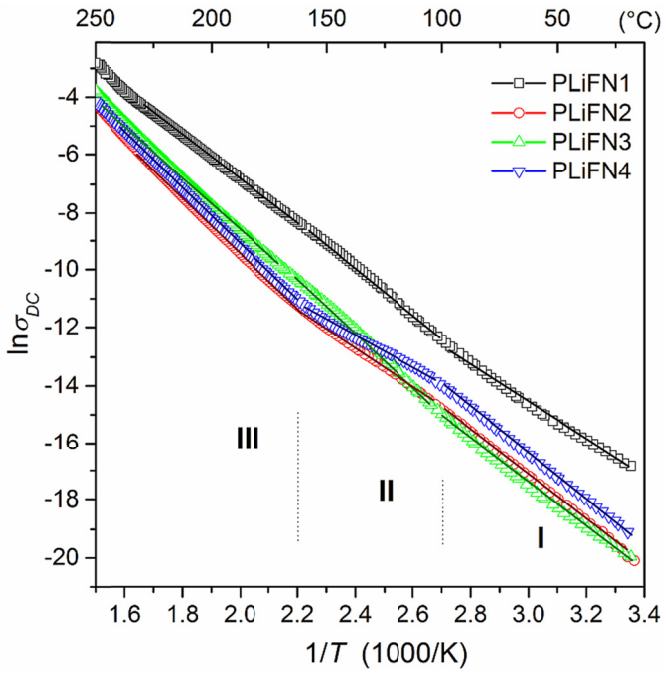

Fig. 6. The $\ln\sigma_{DC}(1/T)$ relationship for the for the PLiFN ceramics

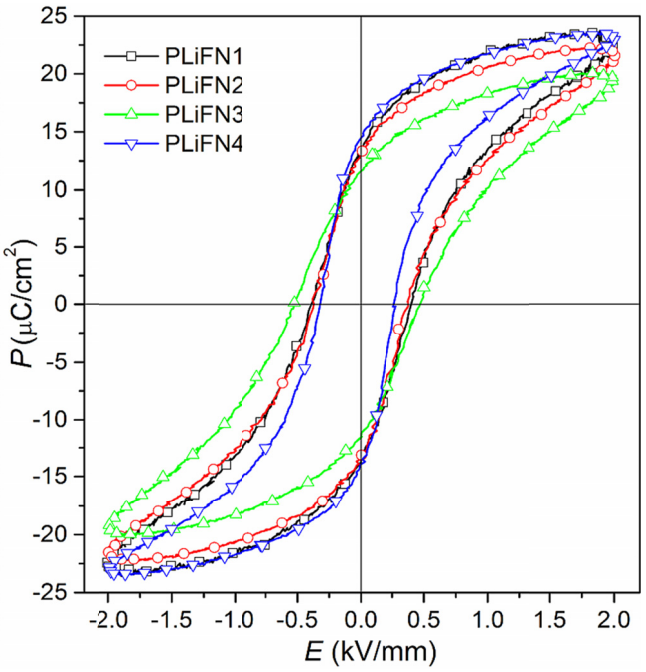

Fig. 7. Hysteresis *P*-*E* loops for PLiFN ceramics (1 Hz, *RT*)

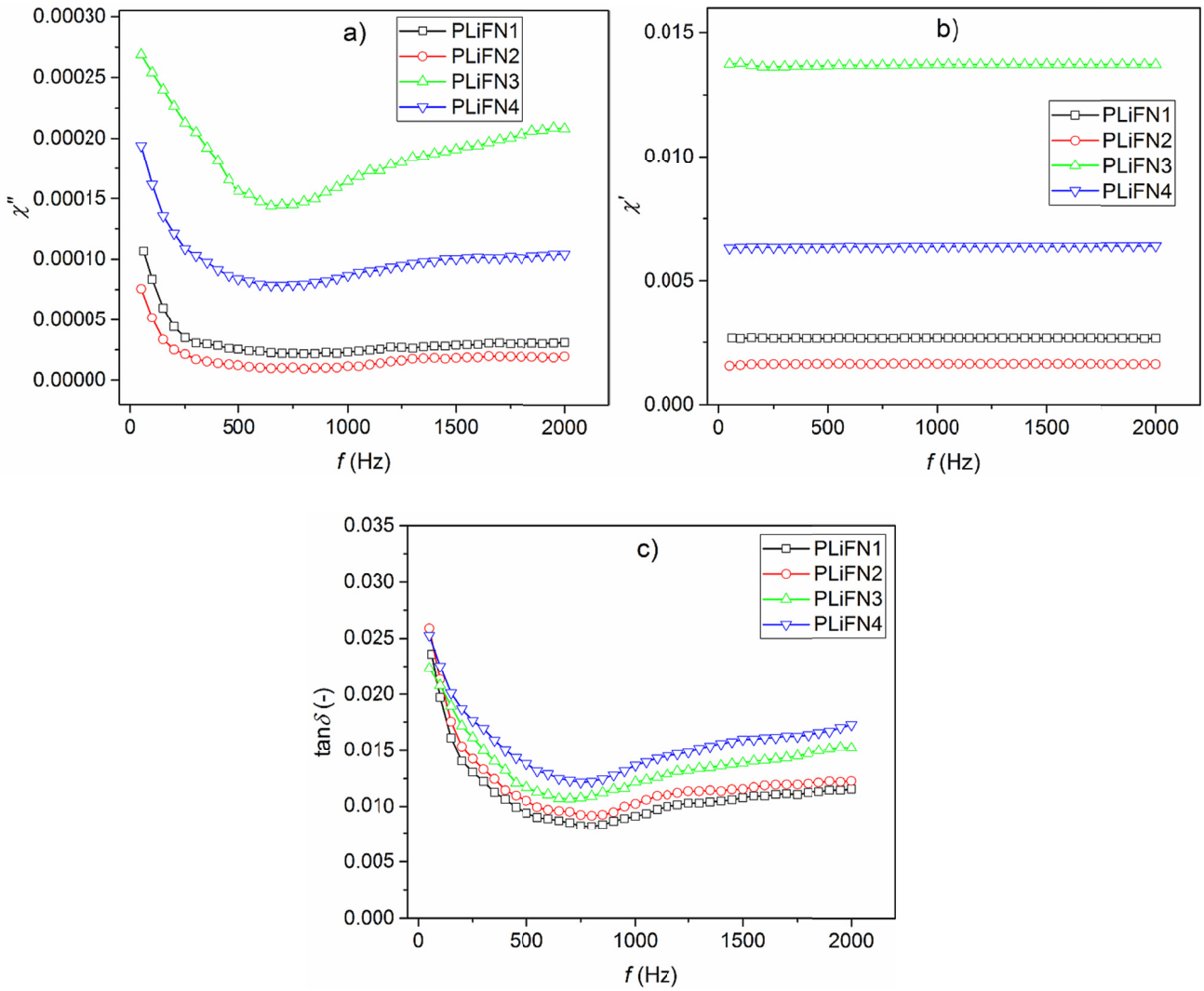

Fig. 8. The dependence of the imaginary (a) and the real (b) part of the susceptibility, and the magnetic loss tangent (c) versus frequency of the magnetic field for PLiFN ceramics sample (at *RT*)

For all samples at the low temperatures (range I) the values of activation energy are lower than the values at the highest temperatures (range II and III). In case of the PLiFN sample sintered at 1150°C the change in the slope of the curve (in the II area – above phase transition) is more pronounced, resulting in a substantial change in the activation energy (Table 2).

The results of *P-E* hysteresis loops investigations (i.e. polarization switching) at room temperature and the frequency 1 Hz are shown in Fig. 7. The PLiFN ceramic samples have good saturated hysteresis loops (characteristic for ferroelectric materials) with E_C coercive field from 0.30 kV/mm to 0.50 kV/mm. The value of P_r remnant polarization is from 11.55 μC/cm^2 to 14.34 μC/cm^2.

Change in dielectric and ferroelectric parameters (dielectric permittivity, remnant polarization and coercive field) of the PLiFN ceramic samples can be explained by the grain size changes and microstructure development as a function of sintering temperature [20]. The increasing grain size reduces the volume fraction of grain boundaries, as well as there is the coupling effect between the grain boundaries and the domain wall decreased, which makes domain reorientation more difficult and constrains the domain wall motion [21].

Fig. 8 shows the imaginary part of the magnetic susceptibility (a), real (b) and the magnetic loss tangent (c) vs. the frequency of the magnetic field (10 Oe = 800 A/m) at *RT*. For all PLiFN samples imaginary part of AC susceptibility (χ'') decreases to a certain point with an increase of frequency of the magnetic field. Then, values of χ'' slowly increases (Fig. 8a). The values of the real part of the magnetic susceptibility (χ') are constant for the entire frequency range (Fig. 8b). The highest values of the χ' have PLiFN3 sample. With increasing frequency of magnetic field the magnetic loss decrease up to approximately 750 Hz for all PLiFN samples. For higher frequencies (range from 750 Hz to 2 kHz), the slightly increase values of the magnetic loss were observed (Fig. 8c). The lowest values of the magnetic loss have a PLiFN1 sample, while the highest occurred for the PLiFN4 sample.

4. Conclusion

In the present paper the ceramic samples of the $PbFe_{1/2}Nb_{1/2}O_3$ material doped by Li (in amount of 5.0% wt.) by the two-stage synthesis (columbite method) were obtained. Comprehensive studies on the influence of synthesis temperature on electrophysical properties, including electrical, dielectric, ferroelectric and magnetic properties of PLiFN ceramic samples were carried out.

XRD investigations have shown that the PLiFN material shown single perovskite phase (i.e. without the pyrochlore phase). The microstructure studies have shown that the addition of lithium (in the amount of 5.0% wt.) and at an appropriate sintering temperature, it positively influences the grain's sizes, shapes and properties. The best microstructure is for PLiFN2 and PLiFN3 samples, thanks to this, these samples have well the electrophysical operational parameters. At room temperature, the PLiFN ceramic samples show both ferroelectric and ferromagnetic properties. Lithium addition decreases the diffusion of phase transition in PFN material and increases the value of dielectric permittivity maximum. With increasing sintering temperature the dielectric permittivity maximum shifts towards lower temperatures. The obtained samples the *P-E* loops are typical for normal ferroelectric materials. Considering the functional parameters of the obtained ceramic samples, the optimal technological conditions are 1100°C/2 h. As a result we conclude that Li-doped PFN ceramics is interesting materials for applications in microelectronic and micromechatronic devices.

REFERENCES

[1] H. Schmid, Ferroelectrics **162**, 317 (1994).
[2] W. Cheong, M. Mostovoy, Nat. Mater. **6**, 13 (2007).
[3] K.F. Wang, J.-M. Liu, Z.F. Ren, Adv. Phys. **58**, 4, 321-448 (2009).
[4] D. Bochenek, J. Alloy. Compd. **504**, 508-513 (2010).
[5] D. Bochenek, J. Dudek, Eur. Phys. J.– Spec. Top. **154**, 19-22 (2008).
[6] G.A. Smolenskii, A.I. Agranovskaia, S.N. Popov, V.A. Isupov, Sov. Phys.-Tech. Phys. 3 1981 (1958).
[7] G.A. Smoleński, W.M. Judin., Fiz. Twierdogo Tela **6**, 3668 (1964).
[8] Y.E. Roginskaya, Y.N. Venevcev, S.A. Fedulov, Sov. Phys. Crystallogr. **8**, 490 (1964).
[9] S. Picozzi et al., J. Phys. – Condens. Matt. **20**, 43, 434208 (2008).
[10] H. Schmid, J. Phys. – Condens. Matt **20**, 43, 434201 (2008).
[11] W. Eerenstein, N. D. Mathur, J. F. Scott, Nature **442**, 759 (2006).
[12] K. Wójcik, K. Zieleniec, M. Mulata, Ferroelectrics **289**, 107 (2003).
[13] D. Bochenek, P. Kruk, R. Skulski, P. Wawrzała, J. Electroceram. **26**, 8-13 (2011).
[14] D. Bochenek, Z. Surowiak, J. Krok-Kowalski, J. Poltierova-Vejpravova, J. Electroceram. **25**, 122-129 (2010).
[15] D. Bochenek, G. Dercz, D. Oleszak, Arch. Metall. Mater. **56**, 4, 1015-1020 (2011).
[16] D. Bochenek**,** Z. Surowiak, J. Alloy. Compd. **480**, 732-736 (2009).
[17] Y. Xu, Ferroelectric materials and their applications, Elsevier, North – Holland, Amsterdam 1991.
[18] R.D. Shannon, Acta Cryst. A **32**, 751-767 (1976).
[19] O. Raymond, R. Font, N. Juarez-Almodovar, J. Portelies, J.M. Siqueiros, J. Appl. Phys. **97**, 084107, 1-8 (2005).
[20] M. Kuwabara, J. Am. Ceram. Soc. **73**, 5, 1438-1439 (1990).
[21] L.B. Kong, J. Ma, Mater. Lett. **51**, 95-100 (2001).